Conformational Change of Bacteriorhodopsin Quantitatively Monitored by Microcantilever Sensors

Thomas Braun,*† Natalija Backmann,* Manuel Vögtli,* Alexander Bietsch,*‡ Andreas Engel,† Hans-Peter Lang,* Christoph Gerber,* and Martin Hegner*

*National Center of Competence for Research in Nanoscale Science, Institute of Physics, and †Maurice E. Müller Institute, Biozentrum, University of Basel, 4056 Basel, Switzerland; and ‡IBM Zurich Research GmbH, 8803 Rüschlikon, Switzerland

ABSTRACT Bacteriorhodopsin proteoliposomes were used as a model system to explore the applicability of micromechanical cantilever arrays to detect conformational changes in membrane protein patches. The three main results of our study concern: 1), reliable functionalization of micromechanical cantilever arrays with proteoliposomes using ink jet spotting; 2), successful detection of the prosthetic retinal removal (bleaching) from the bacteriorhodopsin protein by measuring the induced nanomechanical surface stress change; and 3), the quantitative response thereof, which depends linearly on the amount of removed retinal. Our results show this technique to be a potential tool to measure membrane protein-based receptor-ligand interactions and conformational changes.

INTRODUCTION

Microarray methods are important tools in genomic and proteomic research as well as in disease diagnostics and drug discovery. For the latter, membrane proteins are getting more and more attention and are of primary interest for the pharmaceutical industry (1). The importance of membrane proteins in drug discovery is exemplified by the fact that at least 30% of all known drugs are antagonists for G-protein-coupled receptors (GPCRs) but that current drugs address $<10\%$ of all known GPCRs (2).

Ideally a biosensor for membrane protein receptors should be able to detect two physical changes upon ligand binding: First, the mass increase caused by the ligand and, second, the conformational change of the receptor by which it transmits the signal toward the interior of the cell (3). Further requirements are label-free measurements, real-time data recording, and the possibility of parallelization as a microarray technique.

Conventional label-free methods, such as the surface plasmon resonance imaging technique (SPR; (4)) and quartz crystal microbalance (QCM; (5)), rely on changes of physical properties on the sensor surface. Whereas SPR detects the change of the refracting index on (gold) surfaces, which can be interpreted as mass increase on the sensor surface, QCM directly monitors mass changes. Thus these methods are limited to measuring the mass increase on the sensor surface and can fail if the potential ligand has a low molecular weight (6) as is the case for many ligands of membrane proteins when applied at physiological concentrations. Plasmon waveguide resonance spectroscopy (7) is able to measure protein conformation indirectly and mass changes directly but cannot discriminate between them.

Recently a new micromechanical cantilever-based technique evolved with promising prospects to fulfill all above criteria (8–10). This technique provides a versatile approach for measuring forces on a piconewton scale using cantilevers, small springs with a width and length in the micrometer range, and a thickness typically thinner than 1 μm. The following changes of physical properties taking place on the cantilever surfaces upon analyte binding can be monitored: 1) surface stress-induced bending of the cantilever (static mode); and 2) mass load, leading to changes in the eigenfrequencies of the cantilever (dynamic mode). For membrane protein-based biosensors we envisage, therefore, to detect the ligand binding by dynamic mode and the conformational changes of the membrane protein by static mode (M. Hegner and T. Braun, patent pending, device for detecting characteristics of an organic molecule).

The static mode was successfully applied to detect various biological interactions, such as DNA hybridization (12,13) and protein antibody binding (14,15). The dynamic mode, for which the sensitivity depends on the width of the cantilever resonance (16), has so far been used in gaseous environments or vacuum (17,18). Most recently it has also become possible to use the dynamic mode in liquids and to measure the absolute mass adsorbed on the cantilever accurately in buffer solutions (19). Both measurement methods, static and dynamic mode, can be combined (20).

To investigate the static mode for detection of ligand protein interaction and conformational changes of membrane proteins, we have chosen bacteriorhodopsin (bR) as a model system. This membrane protein was discovered in the early 1970s (21) and is responsible for the photon-driven transport of protons across the purple plasmamembrane of *Halobacteria salinarum*. bR assembles in its native form as a

Submitted August 19, 2005, and accepted for publication January 4, 2006.

Address reprint requests to Martin Hegner, Institute of Physics, NCCR ''Nanoscale Science'', Klingelbergstrasse 82, CH–4056 Basel, Switzerland. Tel.: 41-61-267-37-61; Fax: 41-61-267-37-84; E-mail: martin.hegner@unibas.ch.

© 2006 by the Biophysical Society

0006-3495/06/04/2970/08 $2.00

doi: 10.1529/biophysj.105.072934

two-dimensional (2D) crystal leading to the highest possible density at the cell surface. Structurally and functionally, this protein exhibits high similarities to rhodopsin, the only member of the GPCR protein superfamily with a known structure (22). In contrast to most other GPCRs, both proteins have their ''ligand'' (retinal) covalently bound in their ground state. The photoactive retinal, which is linked by a Schiff base to a lysine, is stabilized by a bundle of seven transmembrane helices (22–24). In rhodopsin this prosthetic group undergoes an 11-*cis* to all-*trans* isomerization after photoadsorption-triggering conformational changes in the protein that lead to the activation of G-proteins. In bR, proton transport is linked to the all-*trans* to 13-*cis* isomerization. This leads to large conformational changes in the protein, which are also documented in the bending of bR crystals (25). Due to the pronounced similarity to GPCRs, its high stability, and availability, bR became the archetype protein to study α-helical membrane proteins in general and GPCRs in particular.

In contrast to rhodopsin of the eye, the retinal in bR is bound to the protein during the complete proton translocation cycle and does not have to be regenerated (26). However, the hydrolysis of the retinal of bR can be emulated by the addition of hydroxylamine, leading to the reaction of the retinal with hydroxylamine to retinaloxime (27). This chemical removal of photoactivated retinal, also called bleaching, is accompanied by structural changes in the bR protein and to the loss of the crystallinity of the bR 2D crystals as demonstrated by atomic force microscopy (AFM; (28)). In comparison with GPCRs in general, this retinal removal can be interpreted as ligand receptor dissociation.

Here we demonstrate the use of microcantilever arrays for the quantitative detection of retinal removal from bR based on the nanomechanical surface stress change.

MATERIAL AND METHODS

Materials

All buffer components were purchased from Sigma-Aldrich (Buchs, Switzerland).

Prebleaching of bR

For all experiments the bR cystein mutant G241C was used (29). The prebleaching of bR was performed at room temperature using a Zeiss Optra light microscope (Oberkochen, Germany) with a band-pass filter (575−625 nm) in a buffer containing 20 mM Tris-HCl, pH 7.2, 100 mM KCl, 0.01% NaN_3, and 200 mM hydroxylamine (28). The sample was cooled with an air ventilator, preventing the sample from heating up significantly during preparation. Time series of different prebleaching states were performed, and the bleached/unbleached ratio of bR molecules was determined by measuring the light absorption at 568 nm using a spectrometer (No. 8453; Agilent, Basel, Switzerland). After photochemical prebleaching the bR proteoliposomes were purified from the hydroxylamine by sedimentation at 8000 rpm in a table centrifuge (Eppendorf Centrifuge 5415, Dr. Vaudois AG, Laussane, Switzerland) for 20 min at 4°C. Then they were resuspended in buffer as described above without hydroxylamine. This cleaning procedure was repeated twice, and the sample was stored overnight at 4°C in the dark.

Functionalization of cantilever arrays

Microfabricated arrays of eight silicon cantilevers of 500 μm length, 100 μm width, 1 μm thickness, and a spring constant of 0.03 N/m were used in all the experiments (Micro- and Nanofabrication group, IBM Zürich Research Laboratory, Rüschlikon, Switzerland).

The cantilever arrays were cleaned in Piranha solution (2 parts concentrated H_2SO_4 96% in 1 part H_2O_2 31%) for 10 min. Subsequently the cantilevers were washed first in a 30% NH_3 solution and then twice in water for 5 min each. The cleaned arrays were coated with 2 nm of Ti (99.99%, Johnson Matthey, London, UK) followed by 20 nm of Au (99.999%, Goodfellow, Bad Nauheim, Germany) using an Edwards L400 e-beam evaporator operated at a base pressure below 10^{-5} mbar and evaporation rates of 0.07 nm/s.

bR proteoliposomes (5 mg/ml) were applied directly onto fresh gold-cantilever interfaces by an ink-jet-spotting MD-P-705-L dispensing system (Microdrop, Norderstedt, Germany) as described previously (30,31). A humidity chamber that allowed stabilizing the relative humidity at >95% prevented the sample from drying. Ten droplets with an estimated volume of 0.1 nl were applied on each cantilever with a spot distance of 50 μm, resulting in a complete wetting of the upper cantilever surface. The cantilevers were incubated for at least 10 min at room temperature (22°C) before washing three times in the buffer described above. In some experiments, cantilevers were skipped during the spotting procedure to obtain a blank reference lever (see section ''Deflection measurements''). The functionalized cantilever arrays were stored in buffer at 4°C for up to 3 days before the deflection experiments were performed.

To characterize the functionalization quality, the cantilevers were washed in H_2O and air dried. Tapping mode AFM (Nanoscope, Multimode 3a, Veeco, Santa Barbara, CA) was used to visualize the proteoliposome coverage across the cantilevers. Imaging cantilevers for tapping mode were purchased from Nanosensors (Neuchatel, Switzerland) ($k = 40$ N/m). The density of the bR patches was estimated by thresholding the height for the lowest bR membrane patch layer directly on the gold, and standard particle analysis routines from the IGOR Pro data analysis environment (Wavemetrics, Portland, OR) were applied. These cantilever arrays were not used for functional membrane protein measurements.

To test the preferential orientation of the bR membrane patches, we performed an immunoassay according to Muller et al. (32). bR membrane patches (1 mg/ml) were physisorbed on ultraflat gold (33) for 25 min at room temperature in a humidity chamber. Surplus material was gently removed by exchanging the buffer (containing 20 mM Tris-HCl, pH 7.2, 100 mM KCl), and immunolabeling was performed with a 100-fold dilution of antiserum 1 mg/ml. After incubation for 1.5 h the gold surface was first washed with buffer, and finally the complete gold was rinsed twice in H_2O and air dried. Visualization was done in tapping mode AFM as described above.

Instrumental setup

A schematic of the experimental setup is shown in Fig. 1 (10).

An eight-cantilever array is mounted in a measuring chamber of ~40 μl. Buffer and reagents can be pumped into the chamber using a syringe pump (Genie Kent, Indulab AG, Gams, Switzerland) at a flow rate of 20 μl/min. The entire setup is placed in a temperature-controlled box that is kept at constant temperature (22.15°C, accuracy ±0.02°C) during the experiment.

The bending of the asymmetrically coated cantilever is read out using a laser beam deflection system: the beam of a vertical cavity surface-emitting laser (wavelength 760 nm, Avalon Photonics, Zürich, Switzerland) is reflected at the apex of the cantilever toward a position sensitive detector (PSD; Sitek, Partille, Sweden). The deflection of the cantilever is recorded versus time.

Deflection experiment

For the in situ bR bleaching experiment on the cantilever, two light-emitting diodes (LEDs) with an emission maximum at 565 nm (L-53SG Super-bright

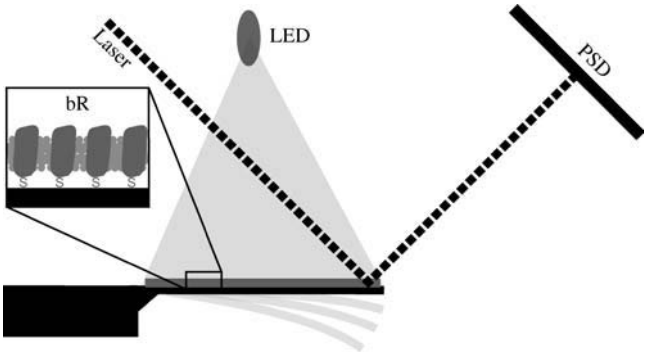

FIGURE 1 Schematic diagram of the setup. bR 2D crystals are immobilized on the upper surface of the cantilever. The deflection of the cantilever is optically detected with a laser using a PSD. To bleach the bR molecules in situ, an LED with an emission maximum at 565 nm was placed above the cantilever. Note that the cystein of the G241C mutant was not essential for membrane anchoring and orientation (see Discussion).

green, Kingbright, Issum, Germany) were installed and powered with 30 mA each (see Fig. 1). This additional light did not interfere with the deflection measurement or change the temperature in the measuring chamber.

Before the bleaching experiment was started, the mechanical properties of the functionalized cantilevers of the array were compared. To this end, a heat test was performed: The measurement chamber containing the cantilever array was heated up by 2°C linearly within 70 s and allowed to cool down again to the working temperature. The asymmetric gold coating forced a compressive bending of the cantilevers due to the different thermal expansion coefficients of gold, titanium, and silicon.

To perform the photochemical reaction and remove the prosthetic retinal from bR, hydroxylamine was injected into the measuring chamber. The cantilever array was constantly illuminated by the LEDs throughout the experiment, otherwise the switching of the LED provoked temperature-induced bending (data not shown), which had to be corrected by corresponding references. The bleaching experiments were performed in three intervals: A baseline was recorded in buffer (20 mM Tris-HCl, pH 7.2, 100 mM KCl, 0.01% NaN_3, section I). To start the bleaching reaction 300 μl of 200 mM hydroxylamine dissolved in the same buffer was injected. After incubation (section II), the hydroxylamine was removed by washing the chamber with 800 μl buffer and the signal after rinsing was recorded (section III).

Data analysis

The IGOR Pro data analysis environment was used for the data processing in four steps: 1), The data were selected according to the heat test performed before the bleaching experiment. Only the data from cantilevers that showed similar mechanical properties were included, which means that only cantilever responses of which the peak maximum differed $<10\%$ were compared to each other. 2), A baseline subtraction was performed for each cantilever over the whole deflection measurement. This was done by linear extrapolation from the baseline recorded before hydroxylamine injection. 3), The data were normalized to the peak maximum of the heating test to minimize the effects of mechanical differences between the cantilevers. To give absolute normalized deflection values, the normalized data were multiplied with the average peak maximum (in nanometers) of the heating test. 4), The differential deflection between sensitized and reference cantilever was calculated. Alternatively, the slope (s) of the deflection change ($s = \Delta d/\Delta t$, where Δd is the deflection change and Δt is the time change) was calculated for certain time points. This was done by a linear regression over the baseline-corrected data.

For the discussion of the involved energy for cantilever bending, the deflection difference between the unbleached and 33% bleached cantilever was determined (see Fig. 5 *A*). Upon saturation, a deflection difference of 180 nm was measured. The differential surface stress between the upper and lower cantilever surface $\Delta\sigma$ was calculated applying Stoney's formula $\Delta\sigma = szET^2/(3L^2(1-\upsilon))$ (34) and the corrections by Sader (35) ($s = 0.83$) to be $\Delta\sigma = 5.35 \times 10^{-2}$ J/m^2 (where z is the deflection; $E = 1.2 \times 10^{11}$ Pa is the Young's module for silicon; $T = 10^{-6}$ m is the cantilever thickness; and $\upsilon = 0.25$ is the Poisson ratio for silicon). In the simplest model, this energy was presumed to be proportional to the number of bR molecules per unit area (Γ) by $\Delta\sigma = \Delta G \times \Gamma$ with ΔG as the Gibbs free energy change per bR protein (34). The density of bR molecules in the proteoliposomes was extrapolated by analyzing Fourier spectra of electron microscope images. The unit cell of the 2D crystal was measured to be 6.3 nm. To calculate the bR density, we assumed that the bR molecules were evenly distributed over the complete cantilever and that only the lower protein layer, which is directly interacting with the cantilever surface, takes part in the mechanical ''signal translation'' process. With 3 bR molecules per unit cell and coverage with bR-containing membrane patches of 90% (Fig. 2), a total of 3.4×10^9 bR molecules per cantilever was estimated.

RESULTS

Functionalization

For the in situ bleaching experiments and deflection measurements, the bR proteoliposomes had to be immobilized on the upper cantilever surface as shown in Fig. 1. This functionalization was performed using an ink jet spotter applying $\sim$1 nl/cantilever. To prevent drying out of the spotted droplets and subsequent denaturation of the membrane proteins, a humidity chamber was built around the cantilever arrays, keeping the cantilever's surface wet for at least 30 min at a relative humidity of $>95\%$.

To determine the membrane protein coverage after spotting, the array was washed with buffer then with water to prevent formation of salt crystals and finally dried in air. Visualization of the proteoliposomes on one of the cantilevers was performed using a tapping mode AFM. Fig. 2 *A* shows a topography image recorded from the functionalized cantilever surface in the center of the cantilever bar. The image reveals typical shapes and sizes of bR proteoliposomes patches and sheets as observed by transmission electron microscopy (data not shown). The corresponding height profile (*panel B*) indicated by the line in panel *A* exhibits height steps of 5 nm.

The coverage of the cantilever with bR derived from a particle analysis routine after height thresholding indicated coverage of $\sim$90%. Only the first bR layer directly on the cantilever was included in these estimations. Incubation time of the cantilever with the spotted droplets containing bR proteoliposomes was at least 10 min for all the experiments. Incubation for a shorter time led to less complete coating.

Immunolabeling the adsorbed bR membrane patches (Fig. 2, *C* and *D*) revealed rough membrane patches similar to the ones observed by Müller et al. (32), indicating a preferential orientation (see Discussion). Only a few unlabeled membrane patches have been observed.

Prebleaching of bR

To explore the linearity of the mechanical signal induced by the in situ bleaching of bR on the cantilever, bR

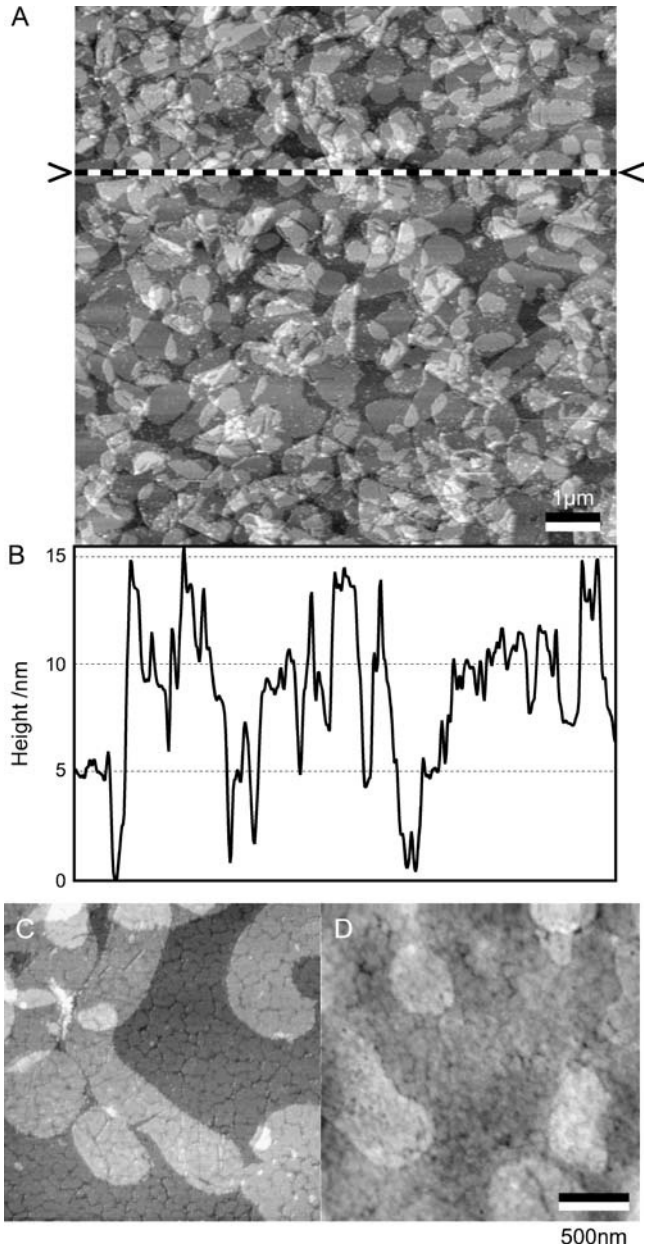

FIGURE 2 Functionalization of the upper cantilever surface with bR membrane patches visualized by tapping mode AFM. The scale bar corresponds to 1 μm. The dashed line, also indicated by two arrowheads in panel *A*, corresponds to the position of the captured height profile (*B*). (*C*) Nonlabeled bR membrane patches immobilized on ultraflat gold (in air, tapping mode). (*D*) Immunoassayed bR patches. Antibodies are specific against the extracellular side of bR, indicating a preferential orientation of bR with the cytoplasmatic side facing the cantilever. Scale bar, 500 nm.

proteoliposomes were partially prebleached in solution before being applied to the cantilever.

Different levels of prebleaching were reached by varying incubation times with 200 mM hydroxylamine and exposition of suspended purple membranes under a light microscope with a band-pass filter in between 570 nm and 620 nm. The samples were incubated for 0, 20, 50, and 110 min, respectively. The absorption spectra, normalized with optical density at 280 nm, are displayed in Fig. 3. With progressive bleaching the absorption peak at 568 nm vanished and a new absorption peak at 360 nm emerged.

The prebleaching grade was estimated from the optical density at the two observed peaks assuming that the sample with longest exposure time is 100% bleached and the unexposed sample is unbleached. The percentage of bleached bR was estimated to be 0%, 33%, 66%, and 100% as indicated in Fig. 3. The initial prebleaching rate was 1.6%/min following a typical saturation curve. The 100% prebleached sample was used for the functionalization of the in situ reference cantilever (see experiment 2 in section ''Deflection measurement'').

Deflection measurements

Two experiments were performed: 1), The deflection of untreated bR was measured versus a blank gold-coated cantilever. 2), bR proteoliposomes with different degrees of prebleaching were used to individually functionalize the cantilevers. In this experiment the differential signal to the reference (functionalized with 100% prebleached bR) was calculated.

In the first experiment, the measurement of bR-sensitized cantilevers versus blank gold cantilevers, the sensitized and reference cantilever (three cantilevers each), were averaged and plotted versus time as depicted in Fig. 4.

The incubation period with hydroxylamine in the measuring chamber is indicated by a gray area (section II of Fig. 4). The error bars indicate the standard deviation for the gold reference (*open circle*) and sensitized cantilever (*solid circle*).

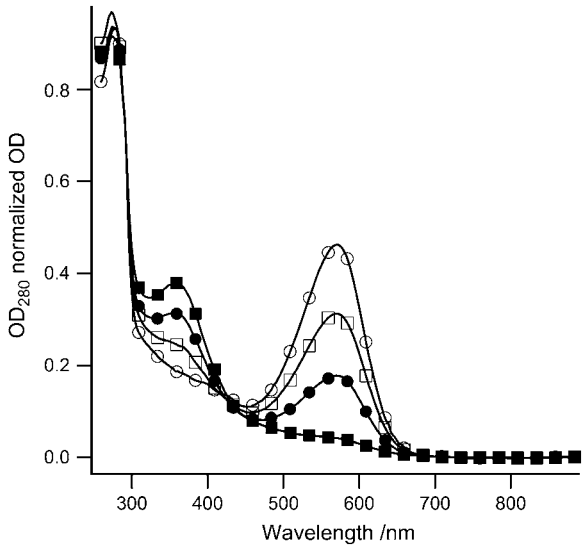

FIGURE 3 Prebleaching of bR crystal before immobilization on the cantilever. The spectra were normalized at 280 nm and the prebleaching grade was determined at 568 nm. Open circles: unbleached; open squares: 33% bleached; filled circles: 66% bleached; and filled squares: 100% bleached. The latter was used to functionalize the reference cantilever.

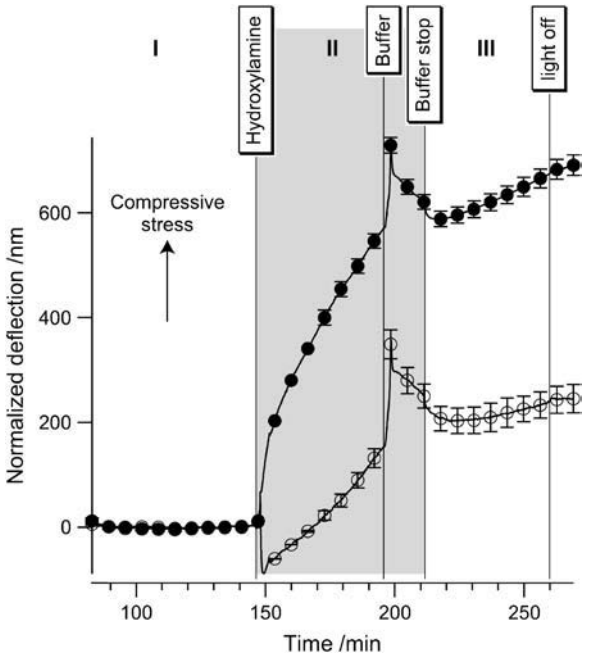

FIGURE 4 Deflection measurement of bR-functionalized cantilevers (*solid circles*) versus blank gold cantilevers (*open circles*). From the 6574 data points, only 30 are labeled and attributed with an error bar indicating the standard deviation of the averaging (three deflection measurements each). Section I, buffer equilibration for baseline; Section II, incubation time with 200 mM hydroxylamine; Section III, after rinsing with buffer. To obtain normalized deflection values (in nanometers), the deflection was first divided with the peak height of the heat test and then multiplied with the average peak height (see Methods).

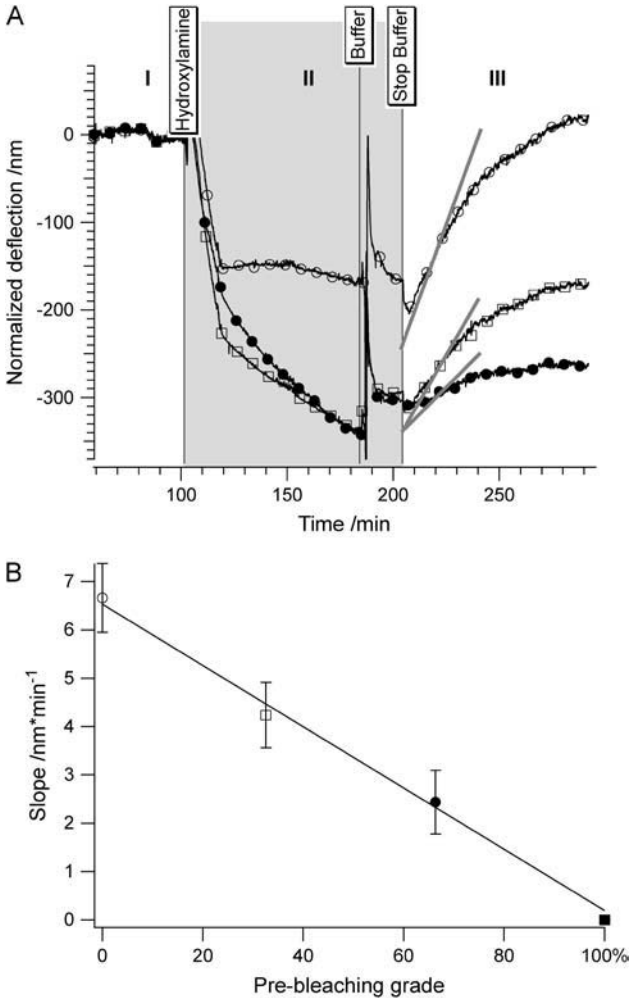

FIGURE 5 (*A*) Differential measurement of cantilever deflection with 100% prebleached bR as reference. The gray area (section II) indicates the injection of hydroxylamine and incubation time where interpretation of the data is complicated by some unspecific interactions (see Discussion). The short gray lines indicate the slopes depicted in panel *B* by linear regression. (*B*) Initial slope after buffer injection versus the prebleaching grade of bR before cantilever functionalization. The slopes were determined between time point 220 and 222 (*A*). The error bars represent the estimated standard deviation of the slope determination. The black line represents a linear regression of the data (Pearson coefficient: $R = -0.99288$). (○) Unbleached; (□) 33% bleached; (●) 66% bleached; (■) 100% bleached (reference in panel *A*).

The deflection measurement shows initially a straight baseline with a standard variation of 1.6 nm for the sensitized and 1.5 nm for the reference cantilever. Immediately after hydroxylamine injection the observed deflection changed significantly. Maximal relative deviations in the deflection of the cantilever of 2.4% only (positive control) or 7.1% (negative control) were observed at the end of the experiment (after 240 min).

After rinsing the chamber with buffer without hydroxylamine, the slope $s = \Delta d/\Delta t$ (where Δd is the deflection change and Δt is the time change) of both the sensitized cantilever and the reference remained different. The first derivative of deflection reflects the relative change independent of any offsets introduced during the incubation time with hydroxylamine. The ongoing deflection change indicates a further progression of the in situ bleaching reaction.

To explore the linearity of the signal, a second experiment was performed. Here, four cantilevers were functionalized with differently prebleached bR 2D crystals as described in section ''Prebleaching of bR''. Cantilevers functionalized with 100% prebleached bR were used as references in these experiments. Fig. 5 *A* displays the differential measurement against the reference.

Incubation in 200 mM hydroxylamine is indicated by the gray area (section II of Fig. 5). The cantilever response proceeds in a very similar way to the experiment shown in Fig. 4: Before the start of the bleaching reaction, fluctuations of 3.5 nm (unbleached), 4.2 nm (33% bleached), and 4.5 nm (66% bleached) in the differential deflection were measured. As in the previous experiment, an immediate change of the cantilever deflection took place after hydroxylamine injection. During the incubation time, sudden deflection changes were regularly observed in different measurements, as is visible in the deflection course of the unbleached bR cantilever in Fig. 5 and the reference cantilever (not shown).

After removing the hydroxylamine by buffer injection, the cantilever deflection change continued in all cantilevers,

reaching saturation after ~1 h. The absolute differential deflection at the end of the experiment is roughly proportional to the prebleaching grade. Due to the instability of the deflection signal during the hydroxylamine injection and incubation, we analyzed the relative changes (s) immediately after the washing step (from 220 to 222 min). In Fig. 5 *B* these slopes are plotted versus the prebleaching grade of bR, resulting in a linear dependence (Pearson coefficient $R = -0.99288$). This finding was reproduced in all experiments performed (data not shown).

DISCUSSION

We present three main results: 1), successful functionalization of micromechanical cantilever arrays with proteoliposomes using ink jet spotting, 2), detection of the removal of the ''ligand'' retinal from the bR protein (bleaching), and 3), quantitative response of micromechanical cantilevers to detect the removal of different amounts of retinal.

Moreover our results demonstrate the applicability of ink jet spotting technology to deposit tiny amounts of functional membrane proteins onto cantilever surfaces. Reproducible cantilever coating with bR proteoliposomes for coverage up to 90% was achieved, documenting the usefulness of this technique. The specific and asymmetrical coating of the cantilever surface by ink jet spotting is mandatory for all subsequent experiments presented here. Gold surfaces are known to be harsh to adsorbed proteins and tend to denature them (see discussion below), but the functionality of the bR protein after immobilization was demonstrated by the subsequent in situ bleaching experiments (see section ''Deflection measurements'').

We used the conditions reported previously for the photobleaching of bR. It was also observed that hydroxylamine can penetrate the bR protein from the extracellular side when immobilized on a surface with the cytoplasmic side (28). A clear difference in deflection development between sensitized and nonsensitized cantilevers was observed during the in situ bleaching reaction (Fig. 4). The low light density of the LED was sufficient for bleaching of the 2D layer of bR proteoliposomes on the cantilever. The small errors between averaged signals of equivalent cantilevers underline the reproducibility of measurements. The fact that the error increases only slightly over time justifies the linear baseline extrapolation for experiments lasting several hours.

In the second bleaching experiment utilizing individually functionalized cantilevers coated with bR proteoliposomes of different degrees of prebleaching, we found linearity in deflection responses (Fig. 5).

In both experiments we observed significant deflection changes immediately after injection and during incubation with hydroxylamine (section II of Figs. 4 and 5). The response of the cantilever during this time interval cannot simply be interpreted as a bleaching reaction. Most likely we also observed unspecific interaction of hydroxylamine with gold (36) as a side effect. These variations have never been detected in experiments, where no hydroxylamine was present.

Immediately after removal of the bleaching agent, we observed a difference between sensitized and reference cantilevers in both the absolute deflection and the relative deflection development (s), revealing a saturation behavior after 60 min. Thus, measuring the slope after the washing step allowed a quantitative interpretation of our data independent of the deflection changes during incubation with hydroxylamine. We provide two possible interpretations for the observed ongoing reaction: 1), After penetration into the protein the hydroxylamine is trapped in a cavity in the bR molecule, enabling it to further react with the Schiff base. This interpretation corroborates the mutant studies demonstrating that the water accessibility of the Schiff base is a rate-limiting step in the hydrolysis reaction and could be accelerated by conformational changes in the bR protein after photon absorption (27). 2), The conformational changes of the proteins are only slowly translated into a global mechanical surface stress change and therefore bending of the cantilever.

The observed deflection changes after removing the hydroxylamine from the measurement chamber are not related to a simple desorption of hydroxylamine: The only difference between the cantilevers is the lacking retinal (see Fig. 5 *A*); therefore, the simplest explanation for the observed correlated deflection change is the bleaching of the immobilized bR molecules.

Our results are in good agreement with the observation of the loss of crystallinity of bR crystals after a bleaching reaction monitored by AFM: There, growing cracks in the crystal with increased degree of bleaching finally leading to the complete loss of crystallinity was observed (28). The degradation of the crystallinity was attributed to structural changes in the individual bR molecules rupturing the protein-protein contacts of the 2D crystal. Therefore, we assume that the measured deflection changes of the cantilever are correlated to structural changes in the membrane protein patches after the bleaching reaction, leading to an expansion of the membrane patches. Thereby a change in the surface tension is expected, forcing a downward bending of the cantilever (compressive stress) since we functionalized only on the upper cantilever surface. This is in good agreement with the observed absolute deflection (see Fig. 4). This finding of the expansion of the proteoliposomes is also corroborated by the current models of the structural changes in the bR helix bundle during the photocycle (37,38): In the M2 state, before relaxation to the ground state, helix F undergoes an outwards movement, opening the proton channel at the cytoplasmatic side.

Labeling with antibodies against the extracellular side of bR membrane patches (32) on annealed gold (33) indicated that most of the proteins are oriented with the cytoplasmatic side toward the cantilever gold (Fig. 2, *C* and *D*). However,

additional experiments comparing Cys mutant bR and wild-type (wt) bR did not reveal significant differences between these two protein forms (data not shown). Therefore we conclude that the Cys modification is not dominating the membrane protein orientation and anchoring of the patches on the cantilever. The observed orientation of bR (wt and Cys mutant) on the gold surface we attribute to the strong negative charge at the cytoplasmatic side forcing mirror charges in the gold, leading to attractive forces. Furthermore, due to the flatness of the bR patches on the gold cantilever we conclude that the bR sheets are not kinetically trapped on the surface and have time to align on the gold to maximize the interactions (39). The generated interactions of the membrane patches with the cantilever interface allow us to transduce surface stress changes into a bending motion.

The question remains whether we are measuring the structural change of the protein itself or whether this change is also correlated to the decay of the crystal order deliberating additional energy that generates force for the bending of the cantilever. The transition observed by Möller et al. resembles the melting of a 2D crystal since with increased bleaching more and more crystal contacts are broken. Phase transitions in this way are in general cooperative processes and not a linear development of the swelling of the membrane patches as expected. Such nonlinear behavior is also clearly indicated by the development of the diffraction patterns (28): The change between the diffraction patterns between a bleaching grade of 10% and 45% is minor (blurring of the diffraction spots), but a significant mosaicity is observed for 70% bleached bR and the diffraction is almost completely lost with a 100% bleached sample. This is not comparable to our data (Fig. 5, *A* and *B*) revealing a linear relationship between bleaching grade and cantilever deflection. Our interpretation of this outcome is that we measure a force transfer of individual bR molecules to the cantilever, indicating that we measure direct changes on the cytoplasmatic side of the bR molecules on the interface. This interpretation of direct translation of protein conformational changes is in line with publication with serotonin-containing cell homogenates (40).

It seems that the conformational changes of bR are linked to the gold surface of the cantilever after retinal removal are irreversible since we have not been able to reconstitute the retinal into the bleached protein on the cantilever interface (data not shown) as described for solution experiments (28). It is known that bR is destabilized after bleaching, as measured by force spectroscopy (41). Our interpretation is that the newly exposed parts of the bR chain physisorb on the gold surface, providing additional energy to the cantilever bending.

Other membrane proteins denatured after direct immobilization on gold surfaces and had to be shielded by a self-assembled organic protection layer to retain their functionality (T. Braun and M. Hegner, unpublished). The potential denaturation of the protein structure may also contribute energy to bending the cantilever by changing the surface stress.

For a more quantitative discussion, the energy per bR molecule contributing to the cantilever bending was estimated (see Materials and Methods): An energy change (in terms of the Boltzmann energy at 295 K) of 195 kT was found for the bleaching reaction for one bR molecule. This calculated energy provides an estimate of the order of magnitude and compares to the energy of a photon of 84 kT with a wavelength of 580 nm, which triggers the photocycle of bR.

The cantilever bending per bR molecule is extrapolated to be 5.5×10^{-18} m. The fluctuations of single cantilevers are <5 nm (see Results). Assuming a minimal deflection difference of at least 10 nm for a clear signal, this means that at least 1.83×10^{8} bR molecules per cantilever have to be activated. This corresponds to 5.5% of all bR molecules on the cantilever.

In our case with bR membrane patches, cantilevers are well suited to ''visualize'' the intrinsic mechanical properties of bR. Taking the high similarity between bR and GPCRs into account, we conjecture that the cantilever-based technique could be able to detect structural changes of these membrane proteins upon ligand binding or unbinding.

CONCLUSIONS

Ten years after the first usage of cantilevers to image the surface of biological membranes at high resolution (42,43), we used micromechanical cantilevers to measure ligand unbinding from membrane proteins based on the intrinsic nanomechanical changes of the receptor.

We thank Joachim Köser (Concentris GmbH, Basel, Switzerland) and Rachel McKendry (London Centre for Nanotechnology, University College London, UK) for fruitful discussions and Georg Büldt (Research Center Jülich, Germany) for biological material.

Financial support is acknowledged from the Swiss National Foundation (National Center of Competence in Research), Commission for Technology and Innovation (Technology Oriented Program (TOP) NANO21), EUCOR Learning and Teaching, Mobility (ELTEM) Nanotechnology project, the IBM Zurich Research Laboratory, and the Roche Research Foundation.

REFERENCES

1. Williams, M. 2003. Target validation. *Curr. Opin. Pharmacol.* 3: 571–577.
2. Wise, A., K. Gearing, and S. Rees. 2002. Target validation of g-protein coupled receptors. *Drug Discov. Today.* 7:235–246.
3. Alberts, B., A. Johnson, J. Lewis, M. Raff, K. Roberts, and P. Walter. 2002. The Molecular Biology of the Cell. Garland Science, New York.
4. Nelson, B. P., T. E. Grimsrud, M. R. Liles, R. M. Goodman, and R. M. Corn. 2001. Surface plasmon resonance imaging measurements of DNA and RNA hybridization adsorption onto DNA microarrays. *Anal. Chem.* 73:1–7.
5. Bizet, K., C. Gabrielli, H. Perrot, and J. Therasse. 1998. Validation of antibody-based recognition by piezoelectric transducers through electroacoustic admittance analysis. *Biosens. Bioelectron.* 13:259–269.
6. Homola, J., S. S. Yee, and G. Gauglitz. 1999. Surface plasmon resonance sensors: review. *Sens. Actuators B Chem.* 54:3–15.

7. Tollin, G., Z. Salamon, and V. J. Hruby. 2003. Techniques: plasmon-waveguide resonance (PWR) spectroscopy as a tool to study ligand-GPCR interactions. *Trends Pharmacol. Sci.* 24:655–659.
8. Gimzewski, J. K., C. Gerber, E. Meyer, and R. R. Schlittler. 1994. Observation of a chemical-reaction using a micromechanical sensor. *Chem. Phys. Lett.* 217:589–594.
9. Thundat, T., R. J. Warmack, G. Y. Chen, and D. P. Allison. 1994. Thermal and ambient induced deflections of scanning force microscope cantilevers. *Appl. Phys. Lett.* 64:2894–2896.
10. Lang, H.-P., M. Hegner, and C. Gerber. 2005. Cantilever array sensors. *Mat. Today.* 8:30–36.
11. Reference deleted in proof.
12. Fritz, J., M. K. Baller, H. P. Lang, H. Rothuizen, P. Vettiger, E. Meyer, H. Güntherodt, C. Gerber, and J. K. Gimzewski. 2000. Translating biomolecular recognition into nanomechanics. *Science.* 288: 316–318.
13. McKendry, R., J. Zhang, Y. Arntz, T. Strunz, M. Hegner, H. P. Lang, M. K. Baller, U. Certa, E. Meyer, H.-J. Güntherodt, and C. Gerber. 2002. Multiple label-free biodetection and quantitative DNA-binding assays on a nanomechanical cantilever array. *Proc. Natl. Acad. Sci. USA.* 99:9783–9788.
14. Arntz, Y., J. D. Seelig, H. P. Lang, J. Zhang, P. Hunziker, J. P. Ramseyer, E. Meyer, M. Hegner, and C. Gerber. 2003. Label-free protein assay based on a nanomechanical cantilever array. *Nanotechnology.* 14:86–90.
15. Backmann, N., C. Zahnd, F. Huber, A. Bietsch, A. Plückthun, H. P. Lang, C. Gerber, and M. Hegner. 2005. Microcantilever-based immunosensor for protein detection using single-chain antibody fragments (scFv). *Proc. Natl. Acad. Sci. USA.* 102:14587–14592.
16. Tamayo, J., A. D. L. Humphris, M. J. Malloy, and A. M. Miles. 2001. Chemical sensors and biosensors in liquid environment based on microcantilevers with amplified quality factor. *Ultramicroscopy.* 86:167–173.
17. Gfeller, K. Y., N. Nugaeva, and M. Hegner. 2005. Rapid biosensor for detection of antibiotic-selective growth of *Escherichia coli*. *Appl. Environ. Microbiol.* 71:2626–2631.
18. Gupta, A., D. Akin, and R. Basjir. 2004. Single virus particle mass detection using microresonators with nanoscale thickness. *Appl. Phys. Lett.* 84:1976–1978.
19. Braun, T., V. Barwich, M. K. Ghatkesar, A. H. Bredekamp, C. Gerber, M. Hegner, and H. P. Lang. 2005. Micromechanical mass sensors for biomolecular detection in a physiological environment. *Phys. Rev. E Stat. Nonlin. Soft Matter Phys.* 72:031907.
20. Battiston, F. M., J. P. Ramseyer, H. P. Lang, M. Baller, C. Gerber, J. K. Gimzewisky, E. Meyer, and H.-J. Güntherodt. 2001. A chemical sensor based on a microfabricated cantilever array with simultaneous resonance-frequency and binding readout. *Sens. Actuators A Phys.* 77:122–131.
21. Oesterhelt, D., and W. Stoeckenius. 1973. Functions of a new photoreceptor membrane. *Proc. Natl. Acad. Sci. USA.* 70:2853–2857.
22. Palczewski, K., T. Kumasaka, T. Hori, C. A. Behnke, H. Motoshima, B. A. Fox, I. Le Trong, D. C. Teller, T. Okada, R. E. Stenkamp, M. Yamamoto, and M. Miyano. 2000. Crystal structure of rhodopsin: a G protein-coupled receptor. *Science.* 289:739–745.
23. Henderson, R., J. M. Baldwin, T. Ceska, F. Zemlin, E. Beckmann, and K. H. Downing. 1990. Model for the structure of bacteriorhodopsin based on high-resolution electron cryo-microscopy. *J. Mol. Biol.* 213: 899–929.
24. Luecke, H., B. Schobert, H. T. Richter, J. P. Cartailler, and J. K. Lanyi. 1999. Structure of bacteriorhodopsin at 1.55 Å resolution. *J. Mol. Biol.* 291:899–911.
25. Porschke, D. 2003. Strong bending of purple membranes in the m-state. *J. Mol. Biol.* 331:667–679.
26. Pepe, I. M. 2001. Recent advances in our understanding of rhodopsin and phototransduction. *Prog. Retin. Eye Res.* 20:733–759.
27. Subramaniam, S., T. Marti, S. J. Rösselet, K. J. Rothschild, and H. G. Khorana. 1991. The reaction of hydroxylamine with bacteriorhodopsin studied with mutants that have altered photocycles: selective reactivity of different photointermediates. *Proc. Natl. Acad. Sci. USA.* 88:2583–2587.
28. Möller, C., G. Büldt, N. A. Dencher, A. Engel, and D. J. Müller. 2000. Reversible loss of crystallinity on photobleaching purple membrane in the presence of hydroxylamine. *J. Mol. Biol.* 301:869–879.
29. Pfeiffer, M., T. Rink, K. Gerwert, D. Oesterhelt, and H. J. Steinhoff. 1999. Site-directed spin-labeling reveals the orientation of the amino acid side-chains in the e-f loop of bacteriorhodopsin. *J. Mol. Biol.* 287:163–171.
30. Bietsch, A., M. Hegner, H.-P. Lang, and C. Gerber. 2004. Inkjet deposition of alkanethiolate monolayers and DNA oligonucleotides on gold: evaluation of spot uniformity by wet etching. *Langmuir.* 12: 5119–5122.
31. Bietsch, A., J. Zhang, M. Hegner, H.-P. Lang, and C. Gerber. 2004. Rapid functionalization of cantilever array sensors by inkjet printing. *Nanotechnology.* 15:873–880.
32. Muller, D. J., C. A. Schoenenberger, G. Büldt, and A. Engel. 1996. Immuno-atomic force microscopy of purple membrane. *Biophys. J.* 70:1796–1802.
33. Hegner, M., and P. Wagner. 1998. Ultraflat AU surfaces. *In* Procedures in Scanning Probe Microscopes. R. J. Colton, A. Engel, J. E. Frommer, H. E. Gaub, A. Gewirth, R. Guckenberger, J. Rabe, W. M. Heckl, B. Parkinson, et al., editors. John Wiley & Sons, Chichester, UK. 169–175.
34. Khaled, A., K. Vafai, M. Yang, X. Zhang, and C. Ozkan. 2003. Analysis, control and augmentation of microcantilever deflections in bio-sensing systems. *Sens. Actuators B Chem.* 94:103–115.
35. Sader, J. 2001. Surface stress induced deflections of cantilever plates with applications to the atomic force microscope: rectangular plates. *J. Appl. Phys.* 89:2911–2921.
36. Tripathi, U. M., W. Scherer, A. Schier, and H. Schmidbauer. 1998. Gold clustering at hydroxylamine. *Inorg. Chem.* 37:174–175.
37. Radzwill, N., K. Gerwert, and H. J. Steinhoff. 2001. Time-resolved detection of transient movement of helices F and G in doubly spin-labeled bacteriorhodopsin. *Biophys. J.* 80:2856–2866.
38. Neutze, R., E. Pebay-Peyroula, K. Edman, A. Royant, J. Navarro, and E. M. Landau. 2002. Bacteriorhodopsin: a high-resolution structural view of vectorial proton transport. *Biochim. Biophys. Acta.* 1565: 144–167.
39. Rivetti, C., M. Guthold, and C. Bustamante. 1996. Scanning force microscopy of DNA deposited onto mica: equilibration versus kinetic trapping studied by statistical polymer chain analysis. *J. Mol. Biol.* 264:919–932.
40. Zhang, Y., S. P. Venkatachalan, H. Xu, X. Xu, P. Joshi, H.-F. Ji, and M. Schulte. 2004. Micromechanical measurement of membrane receptor binding for label-free drug discovery. *Biosens. Bioelectron.* 19:1473–1478.
41. Müller, D. J., M. Kessler, F. Oesterhelt, C. Möller, D. Oesterhelt, and H. Gaub. 2002. Stability of bacteriorhodopsin α-helices and loops analyzed by single-molecule force spectroscopy. *Biophys. J.* 83:3578–3588.
42. Müller, D. J., H. J. Sass, S. A. Muller, G. Büldt, and A. Engel. 1999. Surface structures of native bacteriorhodopsin depend on the molecular packing arrangement in the membrane. *J. Mol. Biol.* 285:1903–1909.
43. Schabert, F. A., C. Henn, and A. Engel. 1995. Native Escherichia coli OmpF porin surfaces probed by atomic force microscopy. *Science.* 268:92–94.